

Tensor Contractions with Extended BLAS Kernels on CPU and GPU

Yang Shi ^{*}, U. N. Niranjan [†], Animashree Anandkumar ^{*}

^{*} EECS Department, [†] ICS Department
University of California, Irvine
Irvine, USA

Email: {shiy4,un.niranjan,a.anandkumar}@uci.edu

Cris Cecka

NVIDIA Research
Santa Clara, USA

Email: ccecka@nvidia.com

Abstract—Tensor contractions constitute a key computational ingredient of numerical multi-linear algebra. However, as the order and dimension of tensors grow, the time and space complexities of tensor-based computations grow quickly. Existing approaches for tensor contractions typically involves explicit copy and transpose operations. In this paper, we propose and evaluate a new BLAS-like primitive STRIDED-BATCHEDGEMM that is capable of performing a wide range of tensor contractions on CPU and GPU efficiently. Through systematic benchmarking, we demonstrate the advantages of our approach over conventional approaches. Concretely, we implement the Tucker decomposition and show that using our kernels yields 100x speedup as compared to the implementation using existing state-of-the-art libraries.

Keywords—Parallelism; BLAS; GPU; Tensor

I. INTRODUCTION

Multi-linear algebraic computations, are ubiquitous in multiple scientific domains such as machine learning and modern data science [3], quantum chemistry and physics [11], signal and image processing [8], chemometrics [6], and biochemistry [10]. *Tensors* are multi-way arrays which can be described as *multi-linear operators*. Tensor contractions play a central role in a variety of algorithms and applications; for a motivating example, see Section II-B. However, non-trivial performance bottlenecks in several application areas are encountered due to the high space and time complexities associated with tensor computations. In this paper, motivated by the recent increased interest from machine learning and deep learning, we propose and study library-based approaches for performing tensor contractions.

Conventional approaches for computing general tensor contractions rely on *matricization*, the logical or explicit restructuring of the data so that the computation can be performed with a sequence of Basic Linear Algebra Subroutine (BLAS) library calls. The BLAS routines provide efficient and portable implementations of linear algebra primitives, with many fast implementations existing across many architectures [7].

The GEneral Matrix Multiply (GEMM) primitive specified within the BLAS library is possibly the most optimized and widely used routine in scientific computing. Noting

that the basic theoretical computational and communication complexities of most tensor contractions is equivalent to that of GEMM, these computations should scale equally well. However, we find that existing tensor libraries such as the TENSOR TOOLBOX and CYCLOPS TENSOR FRAMEWORK perform explicit data transposition to compute almost all tensor contractions and the cost of data restructuring often dominates the cost of the actual computation. In Section III-A, we show that more than 50% of the total evaluation time is taken up in restructuring the data. Other approaches have previously proposed intrusive compiler and static analysis solutions [13], [14], whereas we provide a much simpler library-based solution.

A. Findings and contributions

- We introduce a new BLAS primitive, known as STRIDEDBATCHEDGEMM, that allows the majority of tensor contractions to be computed without any explicit memory motion.
- We demonstrate 5x speedup on CPUs and 20x on GPUs using our approach in direct benchmarks in Section IV-A. In addition, we show 100x speedup in a case study namely, the Tucker decomposition.
- We summarize evaluation guidelines with a pseudocode for performing a single-index tensor contraction without copy or transposition in Algorithm 2.
- We detail the exceptional cases that cannot be evaluated with STRIDEDBATCHEDGEMM and demonstrate that an efficient solution exists with small extension to the primitive.
- The value of this approach is being recognized by NVIDIA. As of this writing, the proposed interface exists in the CUBLAS 8.0 Release Candidate and is likely to appear the official release later this summer.

B. Related Work

Peise *et al* [18] extend results from Napoli *et al* [16] in mapping tensor contractions to sequences of BLAS routines and modeling the performance of these mappings. In this work, they systematically enumerate and benchmark combinations of possible BLAS kernels one could use to

compute a given tensor contraction to conclude that the best performing algorithms involve the GEMM kernel. However, some evaluation strategies, such as *flattening* or developing new, generic linear algebraic subroutines that could yield improved performance, are not considered.

Li *et al* [13] also recognize the cost of explicit copies and propose evaluation strategies exactly comparable to the flattening and batching strategies addressed in this paper. Their discussion of *loop modes* and *component modes* map to our discussion of *batch modes* and *GEMM modes*. However, Li *et al* do not discuss strategies beyond tensor-times-matrix multiply. Furthermore, they only consider *mode- n* tensor-times-matrix contractions of the form $Y_{i_1 \dots i_{n-1} j \dots i_N} = \sum_{i_n} X_{i_1 \dots i_N} U_{j i_n}$, which avoids the more complicated cases in this paper.

The STRIDEBATCHEDGEMM interface proposed in this paper has previously been mentioned by Jhurani *et al* [9] as a low-overhead interface for multiple small matrices on NVIDIA GPUs. Different from their paper that focuses on implementation concerns, in this work, we apply STRIDEBATCHEDGEMM to tensor contraction operations, benchmark evaluation strategies that utilize it, and examine how it may be extended in a multi-linear algebraic library.

The BLAS-like Library Instantiation Software (BLIS) framework [23] offers GEMMs which support non-unit strides in *both* the row and column dimensions. However, the performance is expected to suffer due to decreases in cache line utilization, prefetch bandwidth, and SIMD opportunities.

Recent improvements in parallel and distributed computing systems have made complex tensor computation feasible. TensorFlow [2] can handle multi-linear algebra operations and it is primarily a data-flow and task-scheduling framework for machine learning.

II. BACKGROUND

A. BLAS Routines

BLAS is a set of low-level routines for performing linear algebraic operations. It has three levels namely, vector operations, matrix-vector operations and matrix-matrix operations. We present several standard function documentations in Table I from LAPACK [1]. The ‘s’ in front of the functions specifies single precision data. Since our proposed kernel is based on level-3 BLAS primitive, we will explain the third function in detail: A , B and C are the matrices we operate on and are stored as arrays; TRANS A and TRANS B define the operations on A and B separately (i.e. TRANS A = ‘N’, $op(A) = A$; TRANS A = ‘T’, $op(A) = A^\top$); m and n are the number of rows and columns of the output matrix C ; k specifies the the number of columns of the matrix $op(A)$ (or the number of rows of the matrix $op(B)$); α and β are scalars of the first and second terms in the form; lda ldb and ldc specify the first dimensions of $op(A)$, $op(B)$ and C .

B. Tensor Notation and Preliminaries

We denote tensors by uppercase letters, indices by lower-case letters and index lists by calligraphic letters. We assume all indexing is zero-based. \mathbb{R} denotes the set of real numbers.

The **order** of a tensor is the number of **modes** it admits. A scalar is a zeroth-order tensor, a vector is a first-order tensor, a matrix (say A_{mn}) is a second-order tensor with the rows (indexed by m) being the first mode and columns (indexed by n) being the second mode, and a three-way array (say A_{mnp}) is a third-order tensor with the first, second and third modes indexed by m , n , and p , respectively. Note that we use the term *index* to name a mode and iterate through the elements in that mode.

The **dimension** of the i^{th} mode, denoted $\text{dim}\langle i \rangle$, is the number of elements it contains. The dimension of a mode of a tensor is denoted by the bold lowercase letter of the respective index; for example, the third-order tensor A_{mnp} has dimension $\text{dim}\langle 0 \rangle \times \text{dim}\langle 1 \rangle \times \text{dim}\langle 2 \rangle$ or $\mathbf{m} \times \mathbf{n} \times \mathbf{p}$ where the first mode (indexed by m) takes values $0, \dots, \mathbf{m}-1$, the second mode (indexed by n) takes values $0, \dots, \mathbf{n}-1$, the third mode (indexed by p) takes values $0, \dots, \mathbf{p}-1$.

We follow the Einstein summation convention to represent tensor contractions. A general tensor contraction is written as

$$C_C = \alpha A_{\mathcal{A}} B_B + \beta C_C \quad (1)$$

where $\mathcal{A}, \mathcal{B}, \mathcal{C}$ are ordered sequences of indices such that $\mathcal{C} \equiv (\mathcal{A} \cup \mathcal{B}) \setminus (\mathcal{A} \cap \mathcal{B})$. The indices in $\mathcal{A} \cap \mathcal{B}$ are called *contracted indices*. The indices in \mathcal{C} are called *free indices*.

An Important Practical Application: In unsupervised learning, tensor decomposition [3] is gaining a lot of attention and is the crux of model estimation via the method of moments. A variety of problems such as topic model estimation, Gaussian mixtures model estimation, and social network learning can be provably, consistently and efficiently solved via the tensor decomposition techniques under certain mild assumptions.

The basic building blocks of these algorithms involve tensor contractions. One frequently used tensor decomposition method is the Tucker decomposition [22].

In [24], the authors use the Tucker decomposition to extract new representations of the face images despite different expressions or camera viewpoints. To illustrate the fundamental importance of tensor contractions, we will pick the higher-order orthogonal iteration (HOOI) [12] for asymmetric Tucker decomposition, and use it as a case-study. In the Einstein notation, the factorization of a third-order tensor $T \in \mathbb{R}^{\mathbf{m} \times \mathbf{n} \times \mathbf{p}}$ is given by $T_{mnp} = G_{ijk} A_{mi} B_{nj} C_{pk}$, where $G \in \mathbb{R}^{\mathbf{i} \times \mathbf{j} \times \mathbf{k}}$ is the core tensor, $A \in \mathbb{R}^{\mathbf{m} \times \mathbf{i}}$, $B \in \mathbb{R}^{\mathbf{n} \times \mathbf{j}}$, $C \in \mathbb{R}^{\mathbf{p} \times \mathbf{k}}$. A visualization of a third-order Tucker decomposition is in Figure 1. From Kolda *et al* [21], we summarize the algorithm for the third-order tensor case in Algorithm 1. Following their notation, $T_{(r)}$ denotes the mode- r unfolding

Level	Form	Routines
1	$y = \alpha x + y$	saxpy(n,DA,DX,INCX,DY,INCY)
2	$y = \alpha op(A)x + \beta y$	sgemv(TRANS,m,n,alpha,A,lda,X,INCX,beta,Y,INCY)
3	$C = \alpha op(A)op(B) + \beta C$	sgemm(TRANSA,TRANSB,m,n,k,alpha,A,lda,B,ldb,beta,C,ldc)

Table I: BLAS routines examples

Algorithm 1 Tucker decomposition algorithm.

Require: Tensor $T \in \mathbb{R}^{m \times n \times p}$, core tensor size $\mathbf{i}, \mathbf{j}, \mathbf{k}$, number of iterations \mathcal{T} .

Ensure: Factors A^T, B^T, C^T and core tensor G

```

1: Set  $t = 0$ ;
2: Initialize  $A^0 \leftarrow \mathbf{i}$  leading left singular vector of  $T_{(1)}$ 
    $B^0 \leftarrow \mathbf{j}$  leading left singular vector of  $T_{(2)}$ 
    $C^0 \leftarrow \mathbf{k}$  leading left singular vector of  $T_{(3)}$ 
3: while  $t < \mathcal{T}$  do
4:    $Y_{mjk} = T_{mnp} B_{nj}^t C_{pk}^t$ 
5:    $A^{t+1} \leftarrow \mathbf{i}$  leading left singular vector of  $Y_{(1)}$ .
6:    $Y_{ink} = T_{mnp} A_{mi}^{t+1} C_{pk}^t$ 
7:    $B^{t+1} \leftarrow \mathbf{j}$  leading left singular vector of  $Y_{(2)}$ .
8:    $Y_{ijp} = T_{mnp} B_{nj}^{t+1} A_{mi}^{t+1}$ 
9:    $C^{t+1} \leftarrow \mathbf{k}$  leading left singular vector of  $Y_{(3)}$ .
10: end while
11:  $G_{ijk} = T_{mnp} A_{mi}^T B_{nj}^T C_{pk}^T$ 

```

of tensor T . For further technical details, we refer the reader to Kolda *et al* [21].

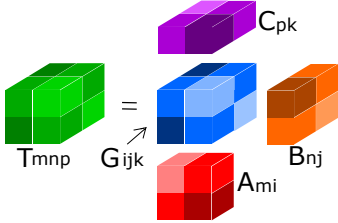


Figure 1: Tucker decomposition

C. Conventional Tensor Contraction

The conventional approach for tensor contraction is to *matricize* the tensors via transpositions and copies. Libraries such as Basic Tensor Algebra Subroutines (BTAS) [15], MATLAB Tensor Toolbox [5], [4], and Cyclops Tensor Framework [20] all perform some version of matricization, which typically involves four steps:

- 1) Consider a general tensor contraction of the form (1). Define the index sets $\mathcal{K}, \mathcal{I}, \mathcal{J}$ as

$$\mathcal{K} = \mathcal{A} \cap \mathcal{B}, \quad \mathcal{I} = \mathcal{A} \setminus (\mathcal{A} \cap \mathcal{B}), \quad \mathcal{J} = \mathcal{B} \setminus (\mathcal{A} \cap \mathcal{B})$$

- 2) Permute tensors A, B , and C into the form

$$C_{\mathcal{I}\mathcal{J}} = \alpha A_{\mathcal{I}\mathcal{K}} B_{\mathcal{K}\mathcal{J}} + \beta C_{\mathcal{I}\mathcal{J}} \quad (2)$$

- 3) Evaluate (2) using one of four BLAS kernels:

$$\begin{cases} \text{DOT} & |\mathcal{K}| = |\mathcal{A}| \text{ and } |\mathcal{K}| = |\mathcal{B}| \\ \text{GER} & |\mathcal{K}| = 0 \\ \text{GEMV} & |\mathcal{K}| = |\mathcal{A}| \text{ xor } |\mathcal{K}| = |\mathcal{B}| \\ \text{GEMM} & \text{else} \end{cases}$$

- 4) Permute the result, $C_{\mathcal{I}\mathcal{J}}$, into the desired output, $C_{\mathcal{C}}$. This approach to tensor contractions is completely general – it works for any two tensors of arbitrary order and any number of contraction indices. However, for even the simplest contractions, the cost of explicitly permuting the tensor data typically outweigh the cost of the computation to be performed. See Section III-A for examples.

III. OUR APPROACH

In this section, we present library-based evaluation strategies for performing general tensor contractions in-place – without explicit copies and/or transpositions.

A. Motivating Observations

Case study: Consider $C_{mnp} = A_{km} B_{pkn}$. The conventional approach presented in Section II-C results in an evaluation wherein we may require more than one transposition. For concreteness, we analyzed how BTAS performs this contraction. We observed that BTAS uses four explicit transpositions that results in the following algorithm:

- 1) Permute A_{km} to A_{mk} .
- 2) Permute B_{pkn} to B_{kpn} .
- 3) Permute C_{mnp} to C_{mpn} .
- 4) Compute $C_{mpn} = \alpha A_{mk} B_{kpn} + \beta C_{mpn}$ with GEMM.
- 5) Permute C_{mpn} to C_{mnp} .

Similarly, in the MATLAB Tensor Toolbox, the main idea is to reshape all tensors to matrices. For instance, in Case 2.4 in Table III, it reshapes A_{km} to A_{mk} and reshapes tensor B_{pkn} to matrix $B_{k(pn)}$ with the first dimension as \mathbf{k} and the second dimension as $\mathbf{p} * \mathbf{n}$. Cyclops also uses index reordering methods for fully dense tensors. The reordering is avoided only in the more restrictive case of high-dimensional symmetric tensors.

We note that some of the steps in the above approach can certainly be avoided with an improved algorithm that still implements the conventional approach. For example, Step 1 can be avoided by using a GEMM that implicitly transposes the first matrix via a TRANSA parameter (from Table I) or equivalent in Step 4. Another optimization would be to avoid Step 3 altogether when $\beta = 0$. Other approaches

require even fewer transposition steps. Ultimately, observe that we may perform the computation without explicit copy by performing p individual GEMMs.

In Figure 2, we measure the cost of these explicit transpose operations in a representative tensor contraction on CPU and GPU. On the CPU we use MKL’s `mkl_somatcopy` and `cblas_sgemm`, and on the GPU we use CUBLAS’s `cublasSgeam` and `cublasSgemm` to perform each required matrix transposition and GEMM respectively.

As we can see from Figure 2, on the CPU, almost 40% of the time is used in copy and transpose, even when only a single mode transposition is performed. Clearly, with more transpose operations, the fraction is higher, requiring 60-80% of the total time. This correlates well with data presented in [13] where it is reported that Tensor Toolbox takes approximately 70% of the total time performing copies and transpositions in one algorithm. Although the fraction of time spent in transposition will asymptotically approach zero as n grows in GPU due to the high bandwidth which allows the computation to dominate the communication, it is clear that the cost of performing explicit copies and transpositions for small tensors, is significant and should be avoided.

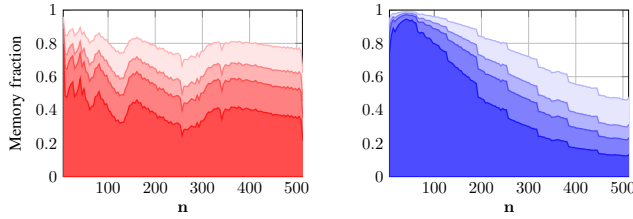


Figure 2: The fraction of time spent in copies/transpositions when computing the contraction $C_{mnp} = A_{mk}B_{pkn}$ using the conventional approach. For color from deep to light: 1, 2, 3, and 6 total transpositions performed on either the input or output. (Left) CPU. (Right) GPU.

B. Extended Notation

We would like to express evaluation strategies for tensor contractions succinctly, so we introduce additional notation.

In this paper, tensors are assumed to be stored in the *column-major* format. In other words, the i^{th} mode has a memory stride – termed “leading dimension” in BLAS – denoted $\text{ld}\langle i \rangle$ with $\text{ld}\langle 0 \rangle = 1$. Using this notation, A_{mnp} is stored as $A[m + n * \text{ld}\langle 1 \rangle + p * \text{ld}\langle 2 \rangle]$. Note that the common *packed-storage* case is obtained when, for all i , we have $\text{ld}\langle i \rangle = \prod_{0 \leq k < i} \text{dim}\langle k \rangle$.

We now formalize three operations that are used in tensor contraction evaluations.

- 1) Batching: $[i]$ denotes that mode i is *batched*, A batched mode is considered *fixed*.
- 2) Flattening: (ij) denotes that modes i and j are *flattened*, i.e., modes i and j are now considered together as

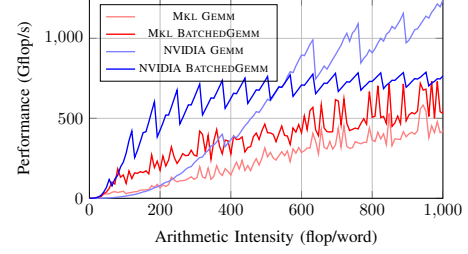


Figure 3: The arithmetic intensity of computing n GEMMs of size $n \times n$ versus the achieved performance on a K40c GPU and 16 cores (32 threads) of a dual socket CPU.

a single mode. The combined mode $h = (ij)$ is considered *free*.

- 3) Transpose: A_{mn}^T denotes a matrix *transpose*. Transposes may only be applied to tensors with exactly two free modes.

The purpose of these notations is that they map directly to looped BLAS calls and the appropriate evaluation can often be read directly from the notated expression. Next, we review some rules that the above notation must follow in order to obtain a well-formed evaluation expression.

- 1) A batched mode $[i]$ cannot be the first mode of any matrix term. That is, $A_{[m]nk}$ is not allowed. Batching in the first mode would cause the m resulting logical $n \times k$ matrices to be strided in both rows and columns and, therefore, cannot be used as a matrix in any BLAS routine.
- 2) A flattening (ij) requires that $\text{ld}\langle j \rangle = \text{ld}\langle i \rangle \text{dim}\langle i \rangle$. Unfortunately, the notation alone is therefore not sufficient to determine which modes may be flattened; it is contingent on the representation as well. In the common packed-storage case, however, this flattening condition is always true.
- 3) If a flattening operation occurs on the right side, it must occur on the left side with the same modes in the same order. For example, $C_{m(np)} = A_{mk}B_{k(pn)}$ is not allowed.
- 4) Standard transposition rules apply: $C_{nm}^T = A_{mk}B_{kn}$ implies $C_{nm} = B_{kn}^T A_{mk}^T$. However, modes may not be swapped under transposition. For example, A_{mk}^T can not be replaced with A_{km} .

This notation allows us to quickly read off the intended extended BLAS evaluation expression for arbitrary tensor contractions. See Table II for examples.

C. BATCHEDGEMM

Instead of relying on explicit mode transpositions, Peise *et al* [17], [18] considered mapping tensor contractions to BLAS primitives directly – enumerating all possible BLAS primitives that could be used and their nesting within loops. Of course, the evaluation strategies that relied on level-3 BLAS primitives (GEMM) rather than level-2 primitives

Contraction	BLAS Evaluation
$C_{m(np)} = A_{mk} B_{k(np)}$	GEMM ('N','N', m , np , k , 1, A , $1da<1>$, B , $1db<1>$, 0, C , $1dc<1>$);
$C_{(mn)p} = B_{(mn)k} A_{pk}^T$	GEMM ('N','T', mn , p , k , 1, B , $1db<1> \cdot 1db<2>$, A , $1da<1>$, 0, C , $1dc<1> \cdot 1dc<2>$);
$C_{m[n]p} = A_{mk} B_{k[n]p}$ for n in $[0, n]$	GEMM ('N','N', m , p , k , 1, A , $1da<1>$, $B + n \cdot 1db<1>$, $1db<2>$, 0, $C + n \cdot 1dc<1>$, $1dc<2>$);
$C_{mn[p]} = A_{k[p]m}^T A_{kn}$ for p in $[0, p]$	GEMM ('T','N', m , n , k , 1, $B + p \cdot 1db<1>$, $1db<2>$, A , $1da<1>$, 0, $C + p \cdot 1dc<2>$, $1dc<1>$);
$C_{[n]p} = B_{pk} A_{k[n]}$ for n in $[0, n]$	GEMV ('N', p , k , 1, B , $1db<1>$, $A + n \cdot 1da<1>$, 1, 0, $C + n$, $1dc<1>$);

Table II: Examples of mappings between tensor contractions with batched and flattened modes in our notation and the corresponding BLAS expression evaluation from Table I. Note that the appropriate BLAS primitive, transposition, matrix pointer, and leading dimension parameters to GEMM can be read off directly from the notation.

(GEMV, GER) were much more efficient. This often resulted in the need for many small GEMMs to be performed, which usually does not achieve ideal performance.

The need to compute many small GEMMs has not gone unnoticed by the leading implementations of BLAS. NVIDIA supplied the capability to multiply pairs of many small matrices in CUBLAS v4.1 [CUDA Toolkit v4.1] via the function `cublasXgemvBatched`. Similarly, as of MKL 11.3 β , `cblas_xgemv_batch` is available with a similar interface and is also optimized for small matrix sizes.

In Figure 3, we plot the achieved performance on CPU and GPU of these BATCHEDGEMM functions by evaluating n GEMMs of size $n \times n$ using each strategy with MKL 11.3.1 and CUBLAS 7.5. Note that there are much higher performance in both cases when n is small. When n is large, there is clearly room for optimization in `cublasSgemvBatched`.

Both of these interfaces are based on pointers to matrix pointers, which often require allocation and/or precomputation at the point-of-call. This makes them awkward to use in the context of tensor contractions where the strides between matrices are regular and the generality provided by these interfaces goes unused.

D. STRIDEDBATCHEDGEMM

Building on the BATCHEDGEMM extensions to BLAS, we propose STRIDEDBATCHEDGEMM which offers a simplified interface for the constant-strided BATCHEDGEMM and more optimization opportunities. The interface and reference implementation of STRIDEDBATCHEDGEMM are provided in Listing 1. The `lda`, `ldb`, `ldc` parameters are the standard “leading dimension” parameters that appear in level-3 BLAS primitives and denote to the stride between columns of the matrix. We refer to the new `loa`, `lob`, `loc` parameters as the “leading order” parameters and denote the stride between matrices of the batch.

There are a number of advantages to a STRIDEDBATCHEDGEMM primitive. First, STRIDEDBATCHEDGEMM is actually more restrictive than the BATCHEDGEMM that has already appeared in MKL and CUBLAS, but we argue that a BATCHEDGEMM with a constant stride between matrices is a common enough case to consider specializing for. By providing this interface,

the common case with constant strides between matrices is not forced to perform allocations or precomputations as it currently must perform in order to use BATCHEDGEMM. Additionally, these extra restrictions provide additional knowledge of the memory layout of the computation and offers additional optimization opportunities in SIMDization, prefetching, and tiling. In other words, the “batch-loop” in STRIDEDBATCHEDGEMM now directly participates in the polyhedral computation as an affine for-loop. With the pointer-interface in BATCHEDGEMM, the “batch-loop” cannot fully participate in a polyhedral model of the computation and is certainly not a candidate for vectorization or cache blocking.

Listing 1: Interface and reference implementation of BLAS-like STRIDEDBATCHEDGEMM.

```

1 // C_p = alpha*opA(A_p)*opB(B_p) + beta*C_p
2 sb_gemm(op_type opA, op_type opB,
3         int m, int n, int k,
4         T alpha,
5         const T* A, int lda, int loa,
6         const T* B, int ldb, int lob,
7         T beta,
8         T* C, int ldc, int loc,
9         int batch_size)
10 {
11     // EXPOSITION ONLY
12     for (int p = 0; p < batch_size; ++p)
13         gemm(opA, opB,
14             m, n, k,
15             alpha,
16             A + p*loa, lda,
17             B + p*lob, ldb,
18             beta,
19             C + p*loc, ldc);
20 }
```

In Table III, we have enumerated all unique single-mode contractions between a second-order and third-order tensor using the notation from Section III-B. All but 8 contractions can be computed with only a single call to STRIDEDBATCHEDGEMM.

IV. RESULTS

In this section, we benchmark varying evaluation strategies in order to define heuristics for computing general tensor contractions without copy or transposition. Additionally,

Case	Contraction	Kernel1	Kernel2	Kernel3	Case	Contraction	Kernel1	Kernel2
1.1	$A_{mk}B_{knp}$	$C_{m(np)} = A_{mk}B_{k(np)}$	$C_{mn[p]} = A_{mk}B_{k[n]p}$	$C_{m[n]p} = A_{mk}B_{k[n]p}$	4.1	$A_{kn}B_{kmp}$	$C_{mn[p]} = B_{km}^\top A_{kn}$	
1.2	$A_{mk}B_{kpn}$	$C_{mn[p]} = A_{mk}B_{k[p]n}$	$C_{m[n]p} = A_{mk}B_{k[p]n}$		4.2	$A_{kn}B_{kpm}$	$C_{mn[p]} = B_{k[p]m}^\top A_{kn}$	
1.3	$A_{mk}B_{nkp}$	$C_{mn[p]} = A_{mk}B_{n[k]p}$			4.3	$A_{kn}B_{mkp}$	$C_{mn[p]} = B_{mk[p]}^\top A_{kn}$	
1.4	$A_{mk}B_{pkn}$	$C_{m[n]p} = A_{mk}B_{p[k]n}$			4.4	$A_{kn}B_{pkm}$	$TRANS(A_{kn}B_{p[k]m}^\top)$	$C_{[m][n]p} = B_{p[k]m}A_{k[n]}$
1.5	$A_{mk}B_{npk}$	$C_{m(np)} = A_{mk}B_{(np)k}$	$C_{mn[p]} = A_{mk}B_{n[p]k}$		4.5	$A_{kn}B_{mpk}$	$C_{mn[p]} = B_{m[p]k}^\top A_{kn}$	
1.6	$A_{mk}B_{pnk}$	$C_{m[n]p} = A_{mk}B_{p[n]k}$			4.6	$A_{kn}B_{pmk}$	$TRANS(A_{kn}B_{p[m]k}^\top)$	$C_{[m][n]p} = B_{p[m]k}A_{k[n]}$
2.1	$A_{km}B_{knp}$	$C_{m(np)} = A_{km}^\top B_{k(np)}$	$C_{mn[p]} = A_{km}^\top B_{k[n]p}$	$C_{m[n]p} = A_{km}^\top B_{k[n]p}$	5.1	$A_{pk}B_{kmn}$	$C_{(mn)p} = B_{k(mn)}^\top A_{pk}$	$C_{m[n]p} = B_{km[n]}^\top A_{pk}$
2.2	$A_{km}B_{kpn}$	$C_{mn[p]} = A_{km}^\top B_{k[p]n}$	$C_{m[n]p} = A_{km}^\top B_{k[p]n}$		5.2	$A_{pk}B_{knm}$	$C_{m[n]p} = B_{k[n]m}^\top A_{pk}$	
2.3	$A_{km}B_{nkp}$	$C_{mn[p]} = A_{km}^\top B_{n[k]p}$			5.3	$A_{pk}B_{mkn}$	$C_{m[n]p} = B_{mk[n]}^\top A_{pk}$	
2.4	$A_{km}B_{pkn}$	$C_{m[n]p} = A_{km}^\top B_{p[k]n}$			5.4	$A_{pk}B_{nkm}$	$TRANS(B_{n[k]m}A_{pk}^\top)$	$C_{[m][n]p} = B_{n[k]m}A_{[p]k}$
2.5	$A_{km}B_{npk}$	$C_{m(np)} = A_{km}^\top B_{(np)k}$	$C_{mn[p]} = A_{km}^\top B_{n[p]k}$		5.5	$A_{pk}B_{mnk}$	$C_{(mn)p} = B_{(mn)k}^\top A_{pk}$	$C_{m[n]p} = B_{m[n]k}^\top A_{pk}$
2.6	$A_{km}B_{pnk}$	$C_{m[n]p} = A_{km}^\top B_{p[n]k}$			5.6	$A_{pk}B_{nmk}$	$TRANS(B_{n[m]k}A_{pk}^\top)$	$C_{[m][n]p} = B_{n[m]k}A_{[p]k}$
3.1	$A_{nk}B_{kmp}$	$C_{mn[p]} = B_{km[p]}^\top A_{nk}$			6.1	$A_{kp}B_{kmn}$	$C_{(mn)p} = B_{k(mn)}^\top A_{kp}$	$C_{m[n]p} = B_{km[n]}^\top A_{kp}$
3.2	$A_{nk}B_{kpm}$	$C_{mn[p]} = B_{k[p]m}^\top A_{nk}$			6.2	$A_{kp}B_{knm}$	$C_{m[n]p} = B_{k[n]m}^\top A_{kp}$	
3.3	$A_{nk}B_{mkp}$	$C_{mn[p]} = B_{mk[p]}^\top A_{nk}$			6.3	$A_{kp}B_{mkn}$	$C_{m[n]p} = B_{mk[n]}^\top A_{kp}$	
3.4	$A_{nk}B_{pkm}$	$TRANS(A_{nk}B_{p[k]m}^\top)$	$C_{[m][n]p} = B_{p[k]m}A_{[n]k}$		6.4	$A_{kp}B_{nkm}$	$TRANS(B_{n[k]m}A_{kp}^\top)$	$C_{[m][n]p} = B_{n[k]m}A_{k[p]}$
3.5	$A_{nk}B_{mpk}$	$C_{mn[p]} = B_{m[p]k}^\top A_{nk}$			6.5	$A_{kp}B_{mnk}$	$C_{(mn)p} = B_{(mn)k}^\top A_{kp}$	$C_{m[n]p} = B_{m[n]k}^\top A_{kp}$
3.6	$A_{nk}B_{pmk}$	$TRANS(A_{nk}B_{p[m]k}^\top)$	$C_{[m][n]p} = B_{p[m]k}A_{[n]k}$		6.6	$A_{kp}B_{nmk}$	$TRANS(B_{n[m]k}A_{kp}^\top)$	$C_{[m][n]p} = B_{n[m]k}A_{k[p]}$

Table III: List of 36 possible single mode contraction operations between a second-order tensor and a third-order tensor and possible mappings to Level-3 BLAS routines. Note that 8 cases may be performed with GEMM, 28 cases may be performed with STRIDEDBATCHEDGEMM, and 8 cases remain exceptional.

Platform	Processor	Properties
CPU	dual-socket Intel Xeon E5-2630 v3 2.4GHz processor	8 cores, 16 threads with an 8×256 KB L2 cache and a 20MB L3 cache per socket
GPU	NVIDIA K40c	2880 streaming cores distributed across 15 multiprocessors and a 1.5MB L2 cache

Table IV: System specifications

we apply and demonstrate the performance of our method on Tucker decomposition.

The system specifications are in Table IV. All data used are randomized dense matrices. To eliminate noise from parallel competition of multi-sockets, all CPU results are generated from serial runs (one core, one thread).

A. Conventional Approach Evaluation

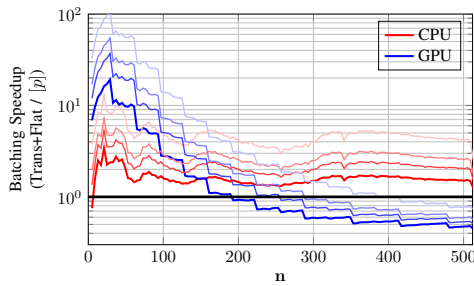


Figure 4: Performance ratio between the conventional approach with κ mode transpositions over a BATCHEDGEMM in $[p]$ for Case 1.3. For color from deep to light, $\kappa = 1, 2, 3, 6$. Performance on CPU using MKL's `mk1_somatcopy`, `cblas_sgemm`, and `cblas_sgemm_batch`. Performance on GPU using CUBLAS's `cublasSgeam`, `cublasSgemm`, and our modified `cublasSgemmBatched`.

We further motivate the use of STRIDEDBATCHEDGEMM

evaluations by plotting the speedup of the batching method over the conventional approach—a single STRIDEDBATCHEDGEMM over transpositions until a single GEMM can be called in evaluation of Case 1.3 from Table III for tensors of size $\mathbf{n} \times \mathbf{n} \times \mathbf{n}$. Figure 4 shows that STRIDEDBATCHEDGEMM is significantly faster than performing even a single transposition followed by a flattened GEMM, especially for small matrices. Here, a single mode transposition means \mathbf{n} calls to `mk1_somatcopy` on CPU or `cublasSgeam` on GPU in order to fully exchange two modes.

On CPU, the STRIDEDBATCHEDGEMM evaluation outperforms the conventional approach for all $\mathbf{n} < 512$ with average 5x speedup. On GPU, for small \mathbf{n} , STRIDEDBATCHEDGEMM has average 20x speedup. The benefit from performing a single flattened GEMM eventually outweighs the cost of performing the transposition and for $\mathbf{n} \gtrsim 200$ the conventional approach achieves a speedup over the STRIDEDBATCHEDGEMM. This speaks to the highly optimized GEMM in CUBLAS and that, perhaps, additional optimization gains from CUBLAS's BATCHEDGEMM may be available.

B. Extended BLAS Evaluation

In this section, we compare evaluation strategies given the extended BLAS kernels. On CPU, the STRIDEDBATCHEDGEMM interface is implemented in serial with looped calls to `cblas_sgemm` from MKL 11.2. On GPU,

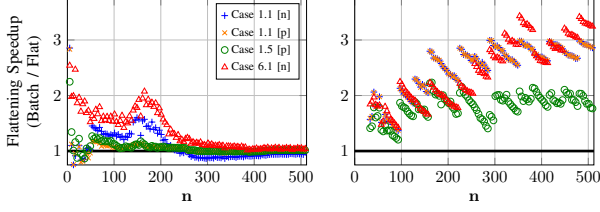


Figure 5: Performance ratio for a BATCHEDGEMM over a flattened GEMM in evaluation of Cases 1.1, 1.5, and 6.1. (Left) CPU. (Right) GPU.

the STRIDEDBATCHEDGEMM interface is provided by modifying `cublasSgemmBatched` from CUBLAS 7.5. Both implementations thereby avoid additional allocation and/or precomputation at the call site. The serial execution on CPU emphasizes the cache effects discussed in the following sections.

1) *Flattening*: Cases 1.1, 1.5, and 6.1 can be evaluated without explicit transpositions with either a single flattened GEMM or a single BATCHEDGEMM. We expect the flattened GEMM evaluation to outperform the BATCHEDGEMM evaluation due to the optimization level of existing GEMMs over that of the recently emerging BATCHEDGEMM functions.

In Figure 5, we plot the speedup achieved by using a flattened GEMM evaluation over a STRIDEDBATCHEDGEMM evaluation. The speedup is greater than one when FlattenedGEMM is faster than the STRIDEDBATCHEDGEMM. Clearly, most of the time, flattened GEMM is faster. Furthermore, we note the CUBLAS implementation of STRIDEDBATCHEDGEMM is a great candidate for optimization as it appears to be significantly underperforming with respect to GEMM.

We also note the dependence of the performance on the shape of the flattened GEMM and the mode of the STRIDEDBATCHEDGEMM. On CPU, we find that the major determining factor in performance is the batching mode of the output. That is, the STRIDEDBATCHEDGEMM evaluation performs best when batched in the third mode of C – in Case 1.5 $[p]$ and 1.1 $[p]$. On GPU, the output batching mode makes no difference. It is unclear why the batched evaluation performs so well on Case 1.5 $[p]$.

2) *Batching*: In this section, we attempt to quantify the performance gain by batching in the last mode versus an earlier mode and whether the input tensor or the output tensor should be prioritized for this optimization.

Case 1.1 and 2.1 can both be batched in the second $[n]$ or third $[p]$ mode. In Figure 6, we plot the speedup in performing the STRIDEDBATCHEDGEMM in $[p]$ over performing it in $[n]$. When $n \lesssim 256$, batching in the third mode is advantageous and can result in up to 1.25x speedup on CPU. When $n \gtrsim 256$, it is approximately 1.1x faster to batch in the second mode rather than the third. We expect this is an effect of the 256KB L1 cache, which

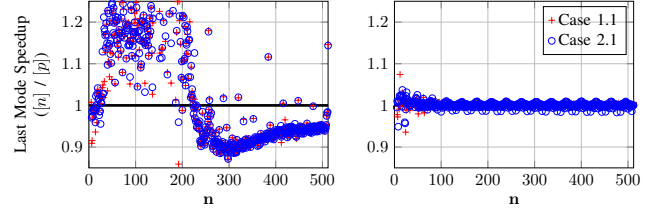


Figure 6: Speedup obtained from batching in the last mode, $[p]$, rather than the middle mode, $[n]$, for Cases 1.1 and 2.1. (Left) CPU. (Right) GPU.

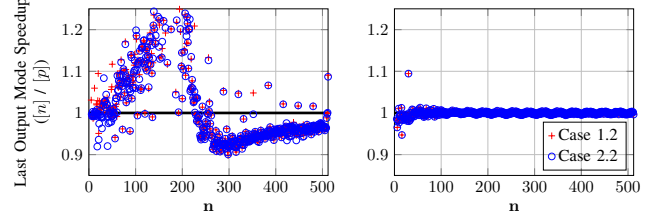


Figure 7: Speedup obtained from batching in the last output mode, $[p]$, rather than the middle output mode, $[n]$, for Cases 1.2 and 2.2. (Left) CPU. (Right) GPU.

would house the contiguous B_{kn} submatrix for each p when $n \lesssim 256$. Beyond that size both batching strategies will have forced cache misses within each GEMM, but by batching in the middle mode more data is shared between individual GEMMs.

On GPU, we see no discernible preference in the choice of batching mode. The GPU has a much less sophisticated memory system with no prefetcher and the performance difference is primarily determined by the number of global memory transactions issued. When $n \geq 32$, the coalescing width is reached so nearly the same number of transactions will be issued in each case – with small differences caused by alignment.

Additionally, we consider the mixed-mode batching evaluations to determine if the input or output array is the primary determination of batching performance. In Figure 7, we plot the speedup in performing STRIDEDBATCHEDGEMM in the last mode of the output but the middle mode of the input, $[p]$, over performing it in the middle mode of the output and the last mode of the input, $[n]$, for Cases 1.2 and 2.2. The results are very similar to those of Figure 6 indicating that batching mode of the output tensor C is more important than the batching mode of the input tensor B on CPU. This is consistent with reference implementations of GEMM which accumulate results directly into the output matrix.

C. Machine Learning Application

In this section, we present the benchmarking results for the application that we discussed in Section II-B. For simulations on the CPU, we compare the performance on the Tucker decomposition using BTAS, CYCLOPS and our

STRIDEBATCHEDGEMM. For simulations on the GPU, we don't have available GPU library to compare with, so we just evaluate our GPU implementation against STRIDEBATCHEDGEMM. We fix the number of iterations as $T = 200$, set the core tensor size as $\mathbf{i} = \mathbf{j} = \mathbf{k} = 10$, and set the dimensions as $\mathbf{m} = \mathbf{n} = \mathbf{p}$. From Figure 8, using our CPU STRIDEBATCHEDGEMM, we obtain more than 10x speedup compared to CYCLOPS and more than 100x speedup compared to BTAS. Also, as expected, our GPU STRIDEBATCHEDGEMM confers further speedup.

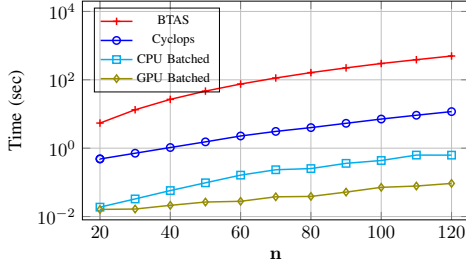


Figure 8: Performance on Tucker decomposition.

V. DISCUSSION AND EXTENSION

According to the results from Section IV, we summarize heuristics and generalizations that can help computation evaluations. Solutions to the exceptional cases will also be discussed in this part.

A. Evaluation Priorities

Rather than attempt to model the algorithm and machine as in [18], [16], we simply provide evaluation guidelines based on the data provided. These are a number of heuristics that may be important in constructing the most efficient evaluation strategy.

- 1) Flatten modes whenever possible. A single large GEMM is more efficient.
- 2) In the interest of performing the highest intensity computation within a STRIDEBATCHEDGEMM, we recommend performing the largest GEMMs possible within a STRIDEBATCHEDGEMM and batching in the mode with largest dimension.
- 3) Preferring to batch in the last mode versus earlier modes can depend on the input parameters and machine.

B. Generalization

In this section, we explain the generality of our approach and how it can be easily applied and extended to single-mode contractions involving tensors of arbitrary order.

Consider an arbitrary single-mode tensor contraction of the form (1). It is straightforward to see by simple counting that the number of unique contractions is $[(|\mathcal{A}| + |\mathcal{B}| - 2)!] \cdot |\mathcal{A}| \cdot |\mathcal{B}|$. We note that Table III is obtained with $|\mathcal{A}| = 2$ and $|\mathcal{B}| = 3$. Of these contractions, all of them may be performed without explicit mode transpositions by nesting the STRIDEBATCHEDGEMM operations.

Algorithm 2 Single-Mode Tensor Contraction

```

1: In: Tensor  $A_{\mathcal{A}}$ ,  $\mathcal{A} = [a_1, \dots, a_M]$ ,
2: In: Tensor  $B_{\mathcal{B}}$ ,  $\mathcal{B} = [b_1, \dots, b_N]$ ,  $\mathcal{A} \cap \mathcal{B} = \{k\}$ .
3: In, Out: Tensor  $C_{\mathcal{C}}$ ,  $\mathcal{C} = [c_1, \dots, c_{N+M-2}]$ . WLOG,  $c_1 \in \mathcal{A}$ .
4: Common substrings in  $\mathcal{A}$ ,  $\mathcal{B}$  and/or  $\mathcal{C}$  for flattening candidates.
5: Relabel flattened modes
6: Compute  $\mathcal{P} = \{c_i \mid i \neq 1, c_i \neq a_1, c_i \neq b_1\}$ 
7: if  $|\mathcal{C} \setminus \mathcal{P}| = |\{c_1\}| = 1$ . then
8:   [Case  $C_{c_1 \dots} = A_{k \dots c_1 \dots} B_{k \dots}$ ]
9:   Let  $c^* \in \mathcal{P} \setminus \mathcal{A}$  be index with max dimension
10:  Let  $c^+ \in \mathcal{P} \setminus \{c_1, c^*\}$  be index with max dimension
11:  Nested in all  $c_j \in \mathcal{P} \setminus \{c^*, c^+\}$ , BATCHEDGEMM in  $c_1, c^*, k, [c^+]$ 
12: else if  $|\mathcal{C} \setminus \mathcal{P}| = |\{c_1, c_b\}| = 2$  then
13:   [Case  $C_{c_1 \dots c_b \dots} = A_{k \dots c_1 \dots} B_{c_b \dots k \dots}$ ]
14:   Let  $c^* \in \mathcal{P}$  be index with max dimension
15:   Nested in all  $c_j \in \mathcal{P} \setminus \{c^*\}$ , BATCHEDGEMM in  $c_1, c_b, k, [c^*]$ 
16: else if  $|\mathcal{C} \setminus \mathcal{P}| = |\{c_1, c_a\}| = 2$  then
17:   [Case  $C_{c_1 \dots c_a \dots} = A_{c_a \dots c_1 \dots k \dots} B_{k \dots}$ ]
18:   Let  $c^* \in \mathcal{P} \setminus \mathcal{A}$  be index with max dimension
19:   Nested in all  $c_j \in \mathcal{P} \setminus \{c^*\}$ , Ex. BATCHEDGEMM in  $c_1, c^*, k, [c_a]$ 
20: else if  $|\mathcal{C} \setminus \mathcal{P}| = |\{c_1, c_a, c_b\}| = 3$  then
21:   [Case  $C_{c_1 \dots c_a \dots c_b \dots} = A_{c_a \dots c_1 \dots k \dots} B_{c_b \dots k \dots}$ ]
22:   Nested in all  $c_j \in \mathcal{P}$ , Ex. BATCHEDGEMM in  $c_1, c_b, k, [c_a]$ 
23: end if

```

We observe that some single-mode contractions of two tensors of arbitrary order can be evaluated by batching on different modes with the STRIDEBATCHEDGEMM operations. For example, consider $C_{mn[p][q]} = A_{mk[p]} B_{nk[q]}$ wherein we can batch in either p and q . We prefer to choose the mode with the larger dimension for the BATCHEDGEMM batching loop over the other (nested batching). This does not negate the need for the exceptional evaluations, which must also be considered for nested batching.

The nested-batching strategy in Listing 2 is general and extends to any two tensors of any order. We summarize these evaluation guidelines with pseudocode for performing a single-index tensor contraction without copy or transposition in Algorithm 2.

Listing 2: Nested batching.

```

1: for (int q = 0; q < Q; ++q)
2:   sb_gemm(OP_N, OP_T,
3:         M, N, K,
4:         1,
5:         A, lda<1>, lda<2>,
6:         B+q*ldb<2>, ldb<1>, 0,
7:         0,
8:         C+q*ldc<3>, ldc<1>, ldc<2>,
9:         P);

```

C. Exceptional Cases

The eight exceptional cases in Table III – Cases 3.4, 3.6, 4.4, 4.6, 5.4, 5.6, 6.4, and 6.6 – occur when batching forces the evaluation to either be a BATCHEDGEMV or violate the no-first-mode rule.

This can be resolved by making an extension to the operation parameters allowed for BATCHEDGEMM. Typically, the available operation parameters are “normal”, “transpose”, “conjugate”, and “Hermitian”. To account for the exceptional cases, “extended X” could be added to allow

violations of the no-first-mode rule and consider all three modes involved in the batching simultaneously.

For example, Case 3.6 and 6.4 could then be written

$$C_{mn[p]} = B_{[p]mk} A_{nk}^\top \quad C_{m[n]p} = B_{[n]km}^\top A_{kp}$$

and evaluated via

```
sb_gemm(OP_EX_N, OP_T,      sb_gemm(OP_EX_T, OP_N,
    M, N, K,                M, P, K,
    1,                      1,
    B, ldb<1>, ldb<2>,      B, ldb<1>, ldb<2>,
    A, lda<1>, 0,           A, lda<1>, 0,
    0,                      0,
    C, ldc<1>, ldc<2>,      C, ldc<2>, ldc<1>,
    P);                      N);
```

When the extended operation is passed, it is known that batching is in the first mode of the input which always has leading dimension 1. Thus, the leading order parameter to `sb_gemm` contains no information. Instead, leading dimensions of the other two modes in row-column order of the batched matrix are passed as the leading dimension and leading order parameters.

The implementation of a computation like this is expected to perform a “3D” tiling of B into cache in order to efficiently contract with the standard 2D cache tiling of A . In the following, we demonstrate the feasibility of evaluation strategies for the exceptional cases.

The Polyhedral Parallel Code Generator (PPCG) [25] is a source-to-source compiler capable of generating CUDA kernels from nested control loops in C. We use PPCG to generate a CUDA kernel for exceptional Case 6.4 and compare its performance against other evaluation strategies.

First, Case 6.4 has four nested loops and PPCG accepts a tiling parameter for each. We search the parameter space $(m, n, p, k) \in [1, 2, 4, 8, 16, 32, 64, 128]^4$ for the most efficient variant in Figure 9. The kernels were generated with $\alpha = 1$ and $\beta = 0$ statically known as generated versions with dynamic α, β had significant branching and divergent overhead, whereas we are primarily interested in the access patterns and tiling.

The tiling parameters that result in the highest performance are $(16, 4, 32, 4)$. Via inspection, we verify that the generated kernel is performing a 2D shared memory tiling for A , a “3D” shared memory tiling for B , and accumulating the C results in registers.

Using the $(16, 4, 32, 4)$ kernel, we benchmark against two possible evaluation strategies: (1) A BATCHEDGEMV which requires no explicit transposition, and (2) A mode transposition in k and m followed by a BATCHEDGEMM in $[n]$. In Figure 10, we show the execution time for each with the explicit transposition/GEMM stacked to show their relative proportion in the two-step evaluation. The PPCG kernel outperforms the explicit transposition/GEMM evaluation for small matrices and remains within a factor of 2-3x as n grows. We expect an expert implementation of the extended transpose parameter kernel would be able to close this gap and remain competitive with BATCHEDGEMM for all n .

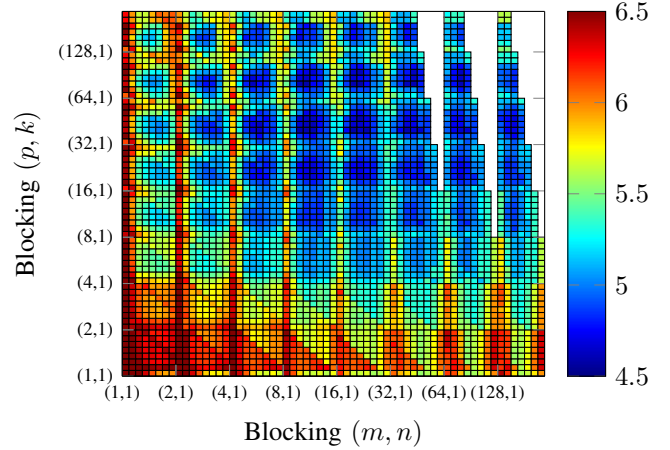


Figure 9: GPU tiling parameter profile from PPCG on K40c for Case 6.4. Performance values are $\log_{10}([\mu\text{sec}])$ and tests performed for $m = n = k = p = 256$. White indicates the run failed.

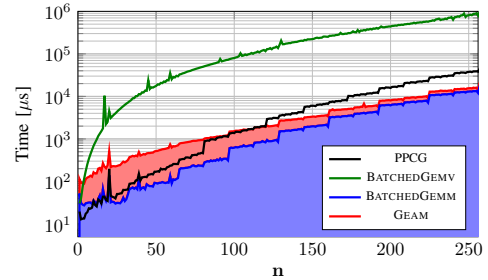


Figure 10: Benchmark of three evaluation strategies for Case 6.4: A BATCHEDGEMV, a mode transposition followed by a BATCHEDGEMM, and an extended transpose kernel generated by PPCG.

VI. CONCLUSIONS AND FUTURE WORK

We propose STRIDEDBATCHEDGEMM and demonstrate its use for generalized tensor contractions. Calls to STRIDEDBATCHEDGEMM have significant opportunity to perform at or near the performance of GEMM by avoiding explicit transpositions or permutations of the data.

We demonstrate that our approach can achieve 5x speedup on CPUs and 20x on GPUs on small and moderate sized tensors. This is very important because in many applications, e.g. deep learning for training a recursive tensor network [19], we require evaluating a large number of tensor contractions of small sizes. To further explain the efficiency of our proposed kernel, we show 100x speedup in the Tucker decomposition. Besides getting performance gains, we also propose a simplified interface that can be then optimized over different platforms.

Further study into the optimized implementations, architecture-dependent implementations, and performance of

the exceptional case kernels is warranted. More complicated contractions, such as multi-index contractions or sparse tensor algebra, also pose challenging problems. We believe that our approach is only a first step in advancing the state-of-the-art multi-linear algebraic computations.

ACKNOWLEDGMENT

The authors would like to thank Aparna Chandramowlishwaran and the UC Irvine HPC Factory lab for providing the computation resources and suggestions. Animashree Anandkumar is supported in part by Microsoft Faculty Fellowship, NSF Career Award CCF-1254106, ONR Award N00014-14-1-0665, ARO YIP Award W911NF-13-1-0084, and AFOSR YIP FA9550-15-1-0221. Yang Shi is supported by NSF Career Award CCF-1254106 and ONR Award N00014-15-1-2737. Niranjan is supported by NSF BigData Award IIS-1251267 and ONR Award N00014-15-1-2737.

REFERENCES

- [1] Lapack-linear algebra package. <http://www.netlib.org/lapack/>. Accessed: 2016-06-13.
- [2] M. Abadi, A. Agarwal, P. Barham, E. Brevdo, et al. TensorFlow: Large-scale machine learning on heterogeneous systems, 2015. Software available from tensorflow.org.
- [3] A. Anandkumar, R. Ge, D. Hsu, S.M. Kakade, and M. Telgarsky. Tensor decompositions for learning latent variable models. *The Journal of Machine Learning Research*, 15(1):2773–2832, 2014.
- [4] Brett W. Bader and Tamara G. Kolda. Algorithm 862: MATLAB tensor classes for fast algorithm prototyping. *ACM Transactions on Mathematical Software*, 32(4):635–653, December 2006.
- [5] Brett W. Bader, Tamara G. Kolda, et al. Matlab tensor toolbox version 2.6. Available online, <http://www.sandia.gov/~tgkolda/TensorToolbox/>, February 2015.
- [6] R. Bro and H. A. Kiers. A new efficient method for determining the number of components in parafac models. *Journal of chemometrics*, 17(5):274–286, 2003.
- [7] Aydin Buluç and John R Gilbert. The combinatorial blas: design, implementation, and applications. *The International Journal of High Performance Computing Applications*, 25(4):496–509, November 2011.
- [8] N. Goyal, S. Vempala, and Y. Xiao. Fourier pca and robust tensor decomposition. In *Proceedings of the 46th Annual ACM Symposium on Theory of Computing*, pages 584–593, 2015.
- [9] C. Jhurani and P. Mulleney. A GEMM interface and implementation on NVIDIA GPUs for multiple small matrices. *Journal of Parallel and Distributed Computing*, 75:133–140, 2015.
- [10] V. Kazeev, M. H. Khammash, M. Nip, and C. Schwab. *Direct solution of the chemical master equation using quantized tensor trains*. ETH-Zürich, 2013.
- [11] V. Khoromskaia and B. N Khoromskij. Tensor numerical methods in quantum chemistry: from hartree–fock to excitation energies. *Physical Chemistry Chemical Physics*, 2015.
- [12] L. De Lathauwer, B. De Moor, and J. Vandewalle. On the best rank-1 and rank- (r_1, r_2, \dots, r_n) approximation of higher-order tensors. *SIAM J. Matrix Anal. Appl.*, 21:1324–1342, 2000.
- [13] J. Li, C. Battaglini, L. Perros, Ji. Sun, et al. An input-adaptive and in-place approach to dense tensor-times-matrix multiply. In *Proceedings of the International Conference for High Performance Computing, Networking, Storage and Analysis*, pages 76:1–76:12.
- [14] Q. Lu, X. Gao, S. Krishnamoorthy, G. Baumgartner, et al. Empirical performance model-driven data layout optimization and library call selection for tensor contraction expressions. *J. Parallel Distrib. Comput.*, 72(3):338–352, Mar 2012.
- [15] N. Nakatani, B. Verstichel, G. Chan, J. Calvin, et al. Btas v0.0.1. Available online, <https://github.com/BTAS/BTAS>.
- [16] E. Di Napoli, D. Fabregat-Traver, G. Quintana-Ort, and P. Bientinesi. Towards an efficient use of the BLAS library for multilinear tensor contractions. *Applied Mathematics and Computation*, 235:454 – 468, 2014.
- [17] E. Peise and P. Bientinesi. Performance modeling for dense linear algebra. In *Proceedings of the 2012 SC Companion: High Performance Computing, Networking Storage and Analysis*. IEEE Computer Society.
- [18] E. Peise, D. Fabregat-Traver, and P. Bientinesi. On the performance prediction of BLAS-based tensor contractions. In *High Performance Computing Systems. Performance Modeling, Benchmarking, and Simulation*. 2015.
- [19] R. Socher, A. Perelygin, J. Wu, et al. Recursive deep models for semantic compositionality over a sentiment treebank. In *Proceedings of the 2013 Conference on Empirical Methods in Natural Language Processing*, pages 1631–1642, Stroudsburg, PA, October 2013.
- [20] E. Solomonik, D. Matthews, J. R Hammond, and J. Demmel. Cyclops tensor framework: reducing communication and eliminating load imbalance in massively parallel contractions. In *Parallel & Distributed Processing*, pages 813–824, 2013.
- [21] G. Kolda Tamara and W. Bader Brett. Tensor decompositions and applications. *SIAM Review*, 51(3):455–500, Mar 2009.
- [22] Ledyard R. Tucker. Some mathematical notes on three-mode factor analysis. *Psychometrika*, 31(3):279–311, 1966.
- [23] Field G. Van Zee and Robert A. van de Geijn. Blis: A framework for rapidly instantiating blas functionality. *ACM Trans. Math. Softw.*, 41(3):14:1–14:33, June 2015.
- [24] M. Alex O. Vasilescu and D. Terzopoulos. Multilinear analysis of image ensemble: Tensorfaces. *ECCV’02*, pages 447–460, 2002.
- [25] S. Verdoolaege, J. C. Juega, A. Cohen, et al. Polyhedral parallel code generation for cuda. *ACM Trans. Archit. Code Optim.*, 9(4):54:1–54:23, January 2013.